

Revealing the Contemporary Kinematics of Antarctic Plate Using GPS and GRACE Data



P. S. Sunil, Ajish P. Saji, K. Vijay Kumar, M. Ponraj, S. Amirtharaj, and Ajay Dhar

Abstract Revised horizontal and vertical plate velocities of the Antarctic continent in ITRF2008 and the impact of elastic and viscoelastic deformations over the continent due to Antarctic Ice Sheet (AIS) variations are simultaneously estimated using GPS and GRACE data for the period 2005–2015. The improved GPS time series and resulting horizontal and vertical velocities indicate that East Antarctica is subsiding significantly, whereas West Antarctica is experiencing uplift with transitional subsidence along the Trans-Antarctic Mountain ranges. According to the ongoing elastic deformation and AIS mass variations from GRACE data, the East Antarctic area is subsiding at a rate of 1 mm/yr. The elastically corrected or GRACE corrected vertical deformation also exposes the deformation patterns associated with the viscoelastic vertical deformation in terms of East Antarctica subsidence and West Antarctica upliftment. The GIA model values also agree well with elastically corrected vertical motions when validated with elastically uncorrected and corrected GPS vertical velocities. Hence we reveal that the outcome of the elastically corrected vertical deformation in the Antarctic region is very well connected to the long-term viscoelastic changes akin to AIS mass variations.

1 Introduction

Antarctica is almost completely encircled by divergent or conservative plate margins, occupying the main plate's unique structural setting (Hayes 1991). However, the lithospheric intra-plate movements taking place in Antarctica can be instigated by various factors. Long-term mass changes in the Antarctic Ice Sheet (AIS) since the Last Glacial Maximum (LGM) cause viscoelastic behavior due to Glacial Isostatic Adjustment (GIA) at first (Farrell 1972). Furthermore, the Earth's crust reacts more

P. S. Sunil (✉)

Department of Marine Geology and Geophysics, CUSAT-NCPOR Centre for Polar Sciences, School of Marine Sciences, Cochin University of Science and Technology, Kochi, India

P. S. Sunil · A. P. Saji · K. V. Kumar · M. Ponraj · S. Amirtharaj · A. Dhar
Indian Institute of Geomagnetism, Mumbai, India

© The Author(s), under exclusive license to Springer Nature Switzerland AG 2022
N. Khare (ed.), *Assessing the Antarctic Environment from a Climate Change Perspective*, Earth and Environmental Sciences Library,
https://doi.org/10.1007/978-3-030-87078-2_18

343

elastically in response to the current mass changes of the AIS. Climate variables such as temperature and humidity control these behaviors associated with snow accumulation and ablation rates on the surface (Huybrechts 1994). The unloading of ice mass can root for slight convergence around the main discharge center in terms of horizontal motions. In contrast, in the case of viscosity, which is an elastic tendency that includes both the lithosphere and the underlying mantle, the divergence obtained is different (Bouin and Vigny 2000).

While conferring the intraplate deformation of the main Antarctic plate, West Antarctica moves independently of East Antarctica during the geological period. The evolution of the western Antarctic and its relationship to the eastern Antarctic have profound implications for the reconstruction of the Gondwana continent, as well as global-scale plate interactions, paleoclimate, and paleo-biogeography (Dalziel and Elliot 1982). Paleomagnetic data suggests that West Antarctica experienced a clockwise rotation of about 175–155 Ma and a counterclockwise rotation of about 155–130 Ma in comparison to East Antarctica (Grunow 1993). As a result, Antarctica can be divided into two structural domains: East Antarctica, which has a stable Precambrian shield, and West Antarctica, which has a more complicated assemblage of accreted terrain (Morelli and Danesi 2004). These two domains are separated by the Transantarctic Mountains (TAM), a 3500 km long-range with elevations up to 4500 m (Brink et al. 1997).

To study the lithospheric dynamics of the Antarctic plate, both, horizontal and vertical displacements of the West and East Antarctic plates must be taken into account. Over the last few decades, geodetic research has focused on calculating the current rate of relative plate motion and comparing it to the rate for millions of years (DeMets et al. 1990; Argus and Heflin 1995). Even though the Antarctic Plate moves/rotates very slowly (Denton et al. 1991; James and Ivins 1998), advances in space geodesy allow for extremely precise and accurate spatial observations in the Polar Regions, particularly in Antarctica, which aid in the study of crustal dynamics, post-glacial rebound, ice mass balance, and other topics (Argus and Peltier 2010; King et al. 2016). The displacement rates of geodetic monuments established over any part of the Earth's surface can be measured with a precision of less than 1 mm/yr using modern space geodetic techniques like very-long baseline interferometry (VLBI), Global Positioning System (GPS), Synthetic Aperture Radar Interferometry (InSAR) etc. and subsequent observations can be compared with predicted values from lithospheric deformation models of the polar regions (Dietrich et al. 2004; Ohzono et al. 2006). In addition, the expansion of Gravity Recovery and Climate Experiment (GRACE) satellite observations conjunction with GPS measurements, which can analyze temporal changes in the Earth's gravitational field and estimates changes in mass near the Earth's surface with incomparable precision, provide the current elastic response of the lithospheric plate with high resolution and accuracy (King et al. 2005; Bevis et al. 2009; Williams et al. 2014).

Contemporary deformation and mass loss of Antarctica is measured using geodetic observations such as the GPS and GRACE measurements, which provide constraints for the GIA model to meet (Dietrich et al. 2004; Ohzono et al. 2006;

Thomas et al. 2011; Williams et al. 2014). Over the Antarctic plate, several continually observing GPS stations are available, especially along the Antarctic coast to assess the elastic crustal deformation in response to the ongoing present-day AIS mass changes, long-term viscoelastic reaction due to GIA, and likely tectonic motion. However, the lack of a network of ground-based GPS observations still limits the vital tasks in the investigation of kinematics and deformation of the Antarctic plate. To address the spatial variation of the Antarctic plate’s contemporary kinematics associated with the present-day ice mass variations, in the present study we use continuous GPS data from 27 permanent GPS stations distributed across the Antarctic continent established by different countries, including the 1 continuous observing GPS stations by India at Maitri (Schirmacher Oasis), and 12 International GNSS Service (IGS) stations (Fig. 1).

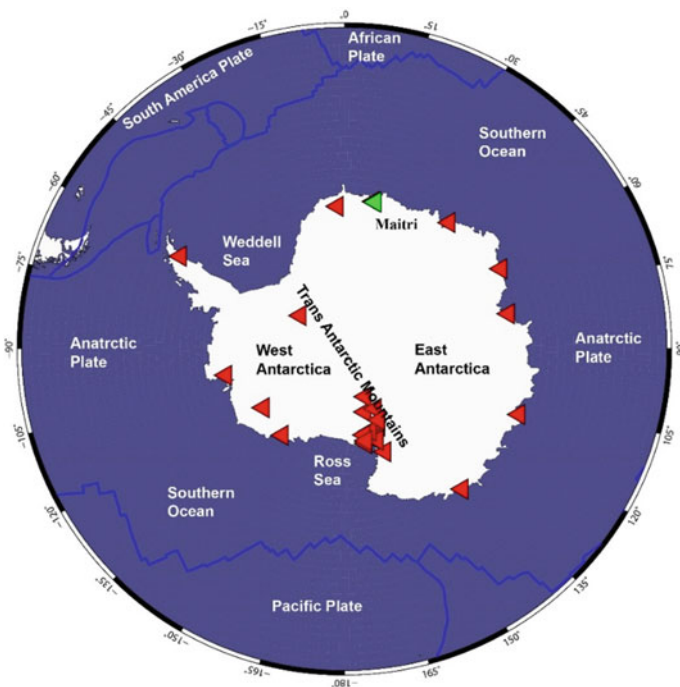


Fig. 1 Map shows the study region Antarctic continent in white color surrounded by the blue color Southern Ocean. The blue lines indicate the plate boundaries of the South Polar Region. The red triangles represent the GPS data used in the present study. The green triangle indicates the location of the Indian Antarctic research base station Maitri

2 Data and Analysis

2.1 GPS Network and Data

We have used continuous GPS data observed from a site (Maitri, established by Indian Institute of Geomagnetism) at the Indian Antarctic research base Maitri at Schirmacher Oasis, East Antarctica, 12 sites from the International GNSS Service (IGS) network, and 14 sites from other national networks during 2005–2015 (Fig. 1). In this study, the data from GPS stations that had been in operation for more than three years were analyzed to achieve accurate results (Blewitt and Lavalle 2002). The GAMIT/GLOBK 10.5 software from (Massachusetts Institute of Technology, USA) is used to obtain the time series of all GPS stations in ITRF2008 (Altamimi et al. 2011). The 24-h GPS dual-frequency and two-phase code observations are used to calculate the daily position (King and Bock 2005; Herring 2005). The first step is to use the satellite orbit parameters published by IGS to eliminate the ionospheric coupling effects through the ionosphere-free linear combinations. In addition, the influence of the Earth tide was corrected using the International Earth Rotation Reference System (IERS2010), and the influence of tidal loads on the ocean was corrected using the finite element solution model (FES2012). The use of sea-bottom pressure models with a time-space resolution of 6 h and 0.5° , respectively, eliminates the effect of non-tidal ocean loading (van Dam et al. 2012). The tropospheric delay correction was employed using a global barometric temperature (GPT) model to estimate zenith delay and horizontal slope (Bohem et al. 2007). The effect of atmospheric loading is derived from the National Center for Environmental Protection (NCEP) reanalysis surface pressure data set. According to the method described in Van Dam and Wahr (1987) and van Dam (2010), this dataset contains daily files of 4 periods with a degree spacing of $2.5^\circ \times 2.5^\circ$. Daily solutions were created by averaging the obtained GPS data sets over 6 h of atmospheric pressure to enable compatibility with the daily solution. The remaining GPS variant time series was then retrieved using two sets of daily solutions (GPS and atmospheric load solutions). In the second step, the computed loose constrained solutions are then passed to GLOBK to estimate the station position, velocity, orbit, and rotation parameters of the Earth using Kalman filtering. We used a set of quality IGS sites to implement the coordinate system in ITRF2008. It is important to note that when processing GPS data using GAMIT/GLOBK, we did not take into account the effects of hydrological or AIS loads; therefore, the surface deformation caused by this effect persists in the remaining GPS time series.

2.2 Common Mode Errors

Common Mode Errors (CME) exist in GPS time series and are one of the major causes of influencing the accuracy and reliability of location coordinates and the

secular variation of GPS locations (Wdowinski et al. 1997; Nikolaidis 2002). The seasonal variations and antenna offsets are the prominent CMEs in the GPS signal. In general, the seasonal signal is modeled by the first and second harmonics of the sine functions, and the model is subtracted from the observed time series. Nikolaidis (2002), Herring (2003), and Tian (2011) proposed the following analytical function to obtain the secular trend, which represents the strain accumulation due to interseismic plate motion:

$$d(t) = c + vt + X \sin(\omega t + \varphi_1) + Y \sin(2\omega t + \varphi_2) + a \left[\ln(1 + t/\tau_{\log}) \text{ or/and } (1 - e^{-(t/\tau_{\exp})}) \right] \quad (1)$$

where $d(t)$ is the displacement as a function of time t , v the linear velocity, c the coseismic offset, X the amplitude of the annual cycle, φ_1 the phase offset of the annual cycle, Y the amplitude of the semi-annual cycle, φ_2 the phase offset of the semi-annual cycle, $\omega = 2\pi/T$, the amplitude of postseismic decay, τ_{\log} the decay time corresponding to logarithmic decay, and τ_{\exp} is the decay time corresponding to exponential decay.

Equation (1) was used to achieve the improved time series and resulting horizontal and vertical velocities containing secular components of tectonic motion. Figure 2 and Fig. 3 show the resultant horizontal and vertical linear/secular motions at all GPS sites in ITRF2008 as calculated using the least-squares method suggested by Tian (2011). The sigmas of the coordinate estimates in the time series are used to calculate the parameter estimates and uncertainties with either white or flicker noise assumptions (Herring 2003). To separate the elastic deformation associated with the contemporary AIS mass changes in the Antarctic region, the GRACE-derived deformation associated with mass fluctuations has been removed from the GPS vertical components.

2.3 GRACE Data

The GRACE satellite's gravity mission was launched in March 2002 to detect mass changes caused by disturbances in the Earth's gravitational field caused by continental hydrology and ice melting (Tapley et al. 2004; Wahr et al. 1998). The errors tracked by GRACE include the total contributions of groundwater, soil water, surface water, snow, ice, and biomass. Based on GPS signals (time series), we used the monthly solution of the field harmonic product GRACE RL03 (Lemoine et al. 2013) of the French organization Groupe de Recherche in Space Geodesy (GRGS). According to Swenson et al. (2008), the center motion coefficient of 1 degree is determined by the Stokes coefficient. To generate outliers, we used the coefficients of the spherical harmonic model and converted the spherical harmonic model to a quality change according to EWH. The spherical harmonics are the 80th and 80th orders, corresponding to a spatial resolution (half-wave) of approximately 250 km

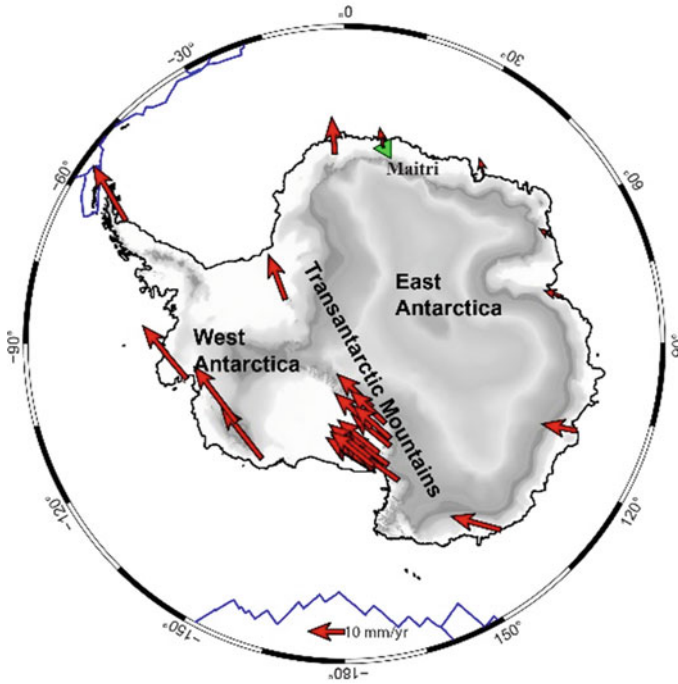


Fig. 2 Map portrays the GPS-derived Antarctic plate horizontal velocity in ITRF2008 after correcting the common-mode errors

(Wahr et al 1998).The inversion of spherical harmonic coefficients of gravity signals yielded vertical and horizontal surface deformations or displacements due to mass variations (Wahr et al., 1998). The horizontal and vertical elastic deformation was described by Farrell (1972) as follows:

$$\Delta H(\theta, \lambda, t) = R \sum_{l=1}^{\infty} \sum_{m=0}^l P_{lm}(\cos\theta) \cdot [\Delta C_{lm}(t)\cos m\lambda + \Delta S_{lm}(t)\sin m\lambda] \cdot \frac{l_l}{1 + k_l} \tag{2}$$

Davis et al. (2004) expressed the vertical elastic deformations as:

$$\Delta V(\theta, \lambda, t) = R \sum_{l=1}^{\infty} \sum_{m=0}^l P_{lm}(\cos\theta) \cdot [\Delta C_{lm}(t)\cos m\lambda + \Delta S_{lm}(t)\sin m\lambda] \cdot \frac{h_l}{1 + k_l} \tag{3}$$

where θ and λ are the latitude and longitude of the observed point at time t , R is the Earth Radius, l and m are the degree and order of the spherical harmonic model,

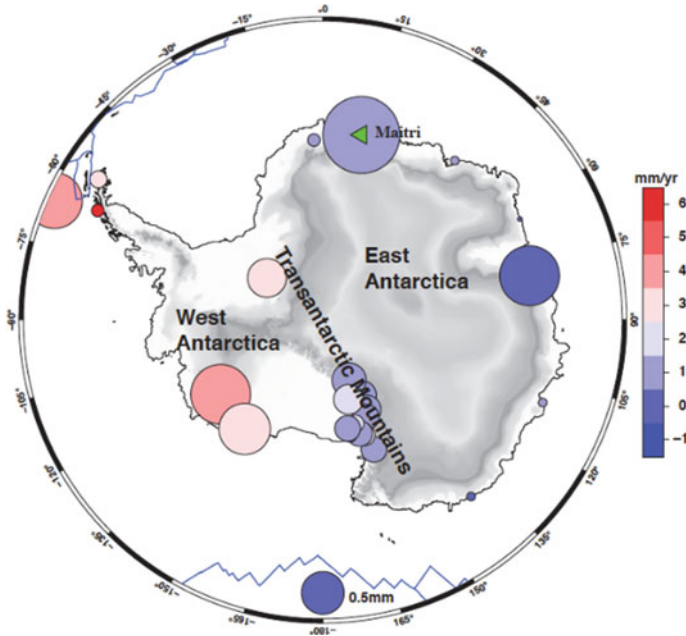


Fig. 3 Map illustrates the GPS-derived Antarctic vertical velocity in ITRF2008 after correcting the common-mode errors. The red shades indicate the uplifting region and blue shades represent the subsidence region. The size of the circles indicates the uncertainty of the GPS-derived vertical rate

P_{lm} is fully normalized Legendre functions, $\Delta C_{lm}(t)$ and $\Delta S_{lm}(t)$ are the spherical harmonic coefficient anomalies of GRACE data and h_l and k_l are elastic Load Love numbers (Pagiatakis 1990). The elastic deformation associated with present-day snow-mass variations was estimated for each GPS location in terms of the Earth-mass centre, as per Eq. (3). We used the Gaussian smoothing on a regional average with a radius of 250 km window and global forward modeling to eliminate correlated GRACE error and bias from GRACE mass changing (Chen et al. 2015). The vertical trend of elastic deformation estimated from the spherical harmonic coefficients of GRACE data over the Antarctic from January 2005 to January 2015 is represented in Fig. 4. The GRACE-derived mass variation-induced displacements in vertical directions are indicated as circles.

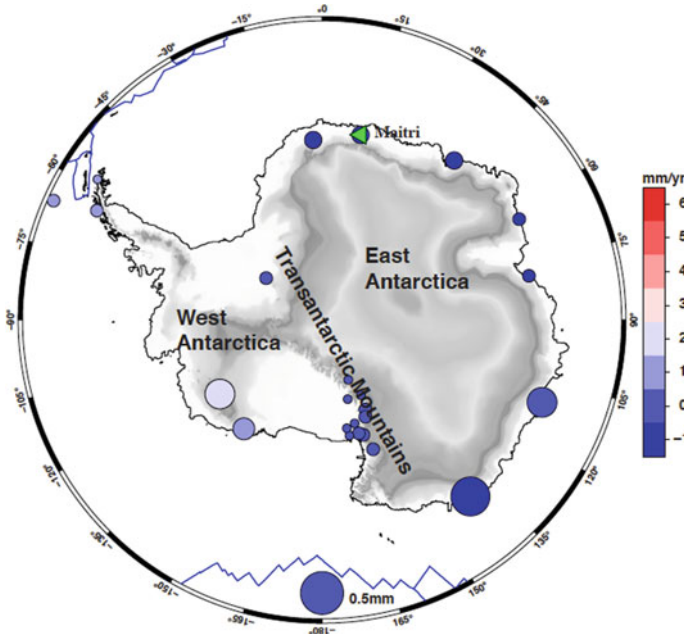


Fig. 4 Map shows the GRACE-derived vertical elastic deformation rate of Antarctica. The red shades indicate the uplifting region and blue shades represent the subsidence region. The size of the circles indicates the uncertainty of the GPS-derived vertical rate

3 Results and Discussion

3.1 GPS-Derived Crustal Motions

Deformations occur in Antarctica due to a combination of factors, including rigid platform rotations, internal tectonic movement, the viscoelastic glacial isostatic adjustment in response to previous ice mass changes, and elastic movement due to present ice mass fluctuations (Farrell 1972; Huybrechts 1994). GPS determined crustal deformation gives a unique proxy record of AIS mass changes due to the Earth’s elastic and viscoelastic response to ice mass accumulations and ablation. The improved time series and resulting horizontal and vertical velocities containing secular components of tectonic motion were obtained using Eq. (1). Preliminary assessment of horizontal and vertical time series GPS and GRACE show that the seasonal variations are present in both horizontal and vertical components, however, the signal is more prominent in vertical displacement. Table 1, Figs. 2 and 3 represent the GPS-derived, both horizontal and vertical deformation pattern of Antarctica.

A tectonic plate motion, viscoelastic, and a local component are included in the measured GPS velocities. The local component is often substantially smaller than

Table 1 Station code, coordinates, improved velocity rates in ITRF2008

Sl. No	Station Code	Latitude	Longitude	North Velocity		East Velocity			
				Rate (mm/yr)	RMS _{raw} (mm)	RMS _{fit} (mm)	Rate (mm/yr)	RMS _{raw} (mm)	RMS _{fit} (mm)
1	BRIP	-75.79	158.46	-12.39	2.2	0.3	08.03	2.2	0.8
2	BURI	-79.14	155.89	-12.30	1.9	0.3	06.13	2.1	0.7
3	CASI	-66.28	110.51	-09.64	2.9	0.2	01.6	3.0	0.5
4	COTE	-77.80	161.99	-12.06	2.1	0.4	08.19	1.9	0.5
5	CRAR	-77.84	166.66	-10.87	1.9	0.2	09.27	2.4	1.2
6	CRDI	-82.86	-053.19	11.11	7.8	6.4	07.12	3.0	0.9
7	DAVR	-68.57	077.97	-04.71	2.3	0.4	-02.87	2.1	0.4
8	DEVI	-81.47	161.97	-12.03	2.1	0.3	06.71	2.3	0.6
9	DUMI	-66.66	140.01	-11.70	3.8	0.4	08.14	4.7	0.8
10	EIG2	-77.53	167.14	-10.13	1.9	0.3	10.14	1.8	0.3
11	FIE0	-76.14	168.42	-11.30	2.4	0.4	10.16	2.2	0.4
12	FLM5	-77.53	160.27	-12.23	1.8	0.2	08.08	1.9	0.7
13	FTP4	-78.92	162.56	-11.98	1.8	0.3	08.03	2.0	0.7
14	HO0Z	-77.53	166.93	-11.40	2.4	0.3	10.80	3.1	0.6
15	IGGY	-83.30	156.25	-12.17	3.6	0.9	05.17	4.5	2.9
16	LWN0	-81.34	152.73	-12.43	2.0	0.6	04.47	2.0	0.6
17	MACZ	-77.53	167.24	-10.38	1.8	0.2	06.20	2.0	0.9
18	MAIT	-70.72	011.50	05.10	2.4	1.1	-02.00	2.7	1.3
19	MAW1	-67.60	062.87	-02.15	2.5	0.3	-03.69	2.4	0.3
20	MCAR	-76.32	-144.30	-04.92	4.7	2.1	17.46	6.2	3.5

(continued)

Table 1 (continued)

Sl. No	Station Code	Latitude	Longitude	North Velocity		East Velocity			
				Rate (mm/yr)	RMS _{raw} (mm)	RMS _{fit} (mm)	Rate (mm/yr)	RMS _{raw} (mm)	RMS _{fit} (mm)
21	MIN0	-78.65	167.16	-11.49	3.5	1.0	09.03	3.6	0.3
22	SCTB	-77.84	166.75	-11.81	2.2	0.3	09.29	2.0	0.4
23	SDLY	-77.13	-125.97	00.63	3.2	0.4	19.35	2.3	0.4
24	SYOG	-69.00	039.58	02.8	2.7	0.4	-03.87	2.7	0.3
25	TOMO	-75.80	-114.66	-11.42	4.3	1.8	05.18	6.5	1.8
26	VESL	-71.67	-002.84	10.25	2.1	0.2	-00.43	2.1	0.4
27	WHN0	-66.01	-060.55	-12.56	2.1	0.2	05.21	2.2	0.4

the plate rotation at intraplate station sites. Thus, in ice-covered regions like Antarctica, the signal emerging from viscoelastic GIA overrules the elastic local signal of deformation. The spatial view of the horizontal velocity map gives a clear picture of the clockwise rotation of the Antarctic continent (Fig. 2). As per the paleomagnetic record, this rotation of the Antarctic plate has been in motion since 175–155 Ma. However, during 155–130 Ma a counter-clockwise rotation was also been recorded (Grunow 1993). Consequences of these past clockwise and counter-clockwise rotations portioned Antarctica into two structural domains, the West and East Antarctica, and these two domains are separated by TAM (Brink et al. 1997; Morelli and Danesi 2004). It may be noted that the horizontal velocity map illustrates that West Antarctica rotates faster than East Antarctica, where the magnitude of the velocity vectors almost doubles compared to East Antarctica. Ghavri et al. (2017) suggested that the Antarctica plate is surrounded by both, convergent and divergence plate margins, hence the plate motions are large in West Antarctica. However, Zanutta et al. (2018) reported that the thickness of the Earth's crust differs between East and West Antarctica, and the intraplate relative velocities calculated from GNSS data demonstrate that movements between the two regions are insignificant.

In terms of GPS-derived vertical deformation (Fig. 3), East Antarctica exhibits significant subsidence while West Antarctica exhibits nearly equal levels of uplift. Nonetheless, the vertical deformation of GPS sites along the TAM indicates a level of subsidence intermediate to that of East Antarctica. It should be noted that the spatial pattern of these velocities does not match any GIA model (Bevis et al. 2009). As a result, the vertical rate estimated from the GPS time series alone cannot be explained by an elastic response to current ice loss. The study, however, supports the existence of discrepancies between the GIA-modeled and observed uplift rates, which could be attributed to deep-seated, regional-scale structures (Zanutta et al. 2018).

3.2 *Elastic Deformation*

For the precise estimation of the viscoelastic behavior due to GIA, the signal separation associated with elastic deformation is critical (King et al. 2012). Because the vertical displacement velocity obtained via GPS analysis is the sum of the GIA-induced viscoelastic and the elastic components. Thus proper correction of elastic deformation is required to extract the GIA-induced crustal deformation with accuracy. Figure 3 shows the GRACE-derived short-term elastic deformation caused by the current AIS mass variation at each GNSS site in this study using Eq. (3). However the horizontal elastic deformation derived using Eq. (2) was negligible, hence here we discuss the results in terms of vertical elastic deformation.

Estimation of the vertical rate of the Antarctic region has been carried out by different investigators. Thomas et al. (2011) and Argus et al. (2014) reported that following the breakaway of the Larsen B Ice Shelf in February 2002, elastic vertical crustal deformation rates in the Northern Antarctic Peninsula dramatically accelerated in response to the abrupt ice mass loss. Lutzow-Holm Bay, part of Drowning

Maud Land, has recently seen a significant increase in surface mass as measured by GRACE (Velicogna et al. 2020). Snowfall has increased in the region recently, as indicated by this mass increase. However, an assessment of GIA solutions based on GPS velocity filed by Li et al. (2019) suggested that GIA and AIS loading have little impact in East Antarctica, where vertical motion is negligible.

In the present study, we calculated the elastic deformation due to the current AIS mass variation at each GPS site using GRACE data. GRACE has recently observed a widespread gain in surface mass over the Antarctica region. The AIS-induced displacements determined from GRACE using Eq. 2 are shown as circles in Fig. 4. According to the estimated deformation, the East Antarctica region experiencing subsidence at a rate of ~ 1 mm/yr due to AIS associated elastic deformation.

3.3 *Elastically-Corrected Deformation*

Seasonal hydrological loading and unloading over continents elastically deform the Earth's surface (Farrell 1972). Seasonal signal contributions from AIS or hydrological mass variations affect the location time series and velocities of GPS stations, as recorded in Antarctica and elsewhere respectively (Blewitt and Lavallée 2002). In order to derive the viscoelastic deformation, we have subtracted the GRACE-derived vertical deformation rates from the GPS-derived counterparts assuming that the remaining vertical deformation in the Antarctic region is associated with the long-term viscoelastic deformation.

In terms of AIS adjusted GPS velocity vectors, Fig. 5 represents the secular rates of the vertical deformation of Antarctica. The GRACE corrected vertical deformation, exposes two unique deformation patterns of eastern side subsidence and western side upliftment. It may be noted that the maximum upliftment is taking place in West Antarctica and especially in the Antarctic Peninsula region. As reported by (Hattori et al. 2021), here, we believe that these corrections are the vertical motion of GIA due to changes in the viscoelastic AIS mass variations. Thus the results highlight the GIA-induced vertical trend of the Antarctic continent. It is also worth mentioning that the GIA's ice-sheet margin forecasts are heavily reliant on ice-sheet models. To further analyze the disparities in the GPS-derived and modeled GIA signals, additional GIA model estimates using alternative ice models are necessary.

3.4 *Validation with GIA Model*

A numerical simulation of global glacial isostatic adjustment is referred to as a GIA model. ICE-6G_C (VM5a) is a novel model (Argus et al. 2014) of the Late Quaternary ice age's last deglaciation episode (Fig. 6). Compared to the previous GIA models, ICE-6G_C (VM5a) model has been explicitly refined by applying all available GPS

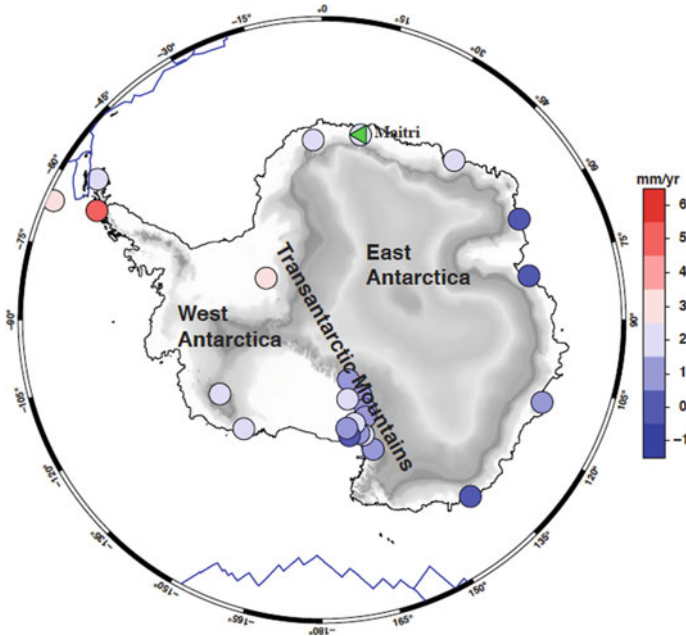


Fig. 5 Map represents the elastically corrected (i.e. GPS minus GRACE) vertical deformation rate of Antarctica. The red shades indicate the uplifting region and blue shades represent the subsidence region

measurements of vertical crustal motion that can be used to constrain the thickness of local ice cover and its removal timing.

In order to evaluate the correlation between the vertical velocities of the elastically uncorrected and corrected GPS values and the prediction of GIA model (ICE-6G_C [VM5a]), we present a linear fit between the vertical velocity of the GPS station and the predicted value of each GIA model in Fig. 7. It may be noted that the linear fit of the annual vertical amplitude of the GPS-GRACE (i.e. elastically corrected) values better fit with the GIA model (slope = 0.86; correlation coefficient = 0.83) compared to the fit of elastically uncorrected GPS velocities (slope = 0.78; correlation coefficient = 0.75). I.e. higher the correlation coefficient, the larger the degree of coincidence between the vertical velocities measured at GPS stations and the GIA model’s predictions. This indicates that the elastically corrected (GPS–GRACE) site velocities are in best agreement with the GIA model velocities. The differences in the observations and model can be ascribed to ice-load histories, different computation methodologies, and earth model parameters (Groh et al. 2012).

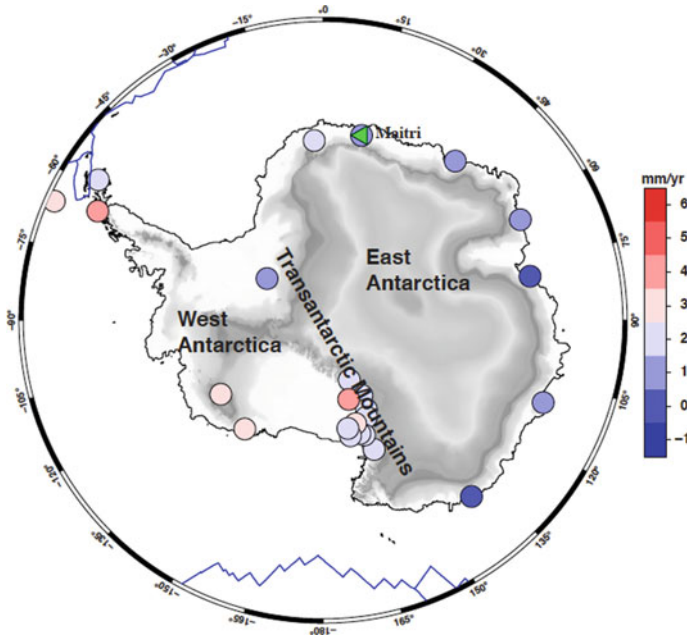


Fig. 6 Map illustrates the GIA model (ICE-6G_C [VM5a]) estimates of the vertical crustal motion values at the GPS locations used in the present study. The red shades indicate the uplifting region and blue shades represent the subsidence region

4 Conclusions

In regions like Antarctica, the short-term elastic response from current mass changes, the long-term viscoelastic impact from ice-sheet mass variations, and sometimes ongoing tectonic processes all work together to create horizontal and vertical crustal displacements. These short and long-term deformations can be captured very precisely with continuous GPS monitoring. The separation of these signals, on the other hand, is critical. In terms of Antarctic tectonic plate motion, the improved GPS time series and resulting horizontal and vertical velocities demonstrate that East Antarctica is subsiding significantly, whereas West Antarctica is experiencing almost equal uplift with transitional subsidence along the TAM regions. However, according to ongoing elastic deformation and current AIS mass fluctuations from GRACE data, the East Antarctic area is subsiding at a rate of 1 mm/yr. To derive long-term viscoelastic deformation GRACE-derived vertical elastic deformation rates were subtracted from GPS-derived equivalents. Further, the elastically adjusted or GRACE corrected vertical deformation highlights the deformation patterns in terms of East Antarctica subsidence and West Antarctica upliftment associated with the long-term viscoelastic vertical deformation. The validation of the GIA model with elastically

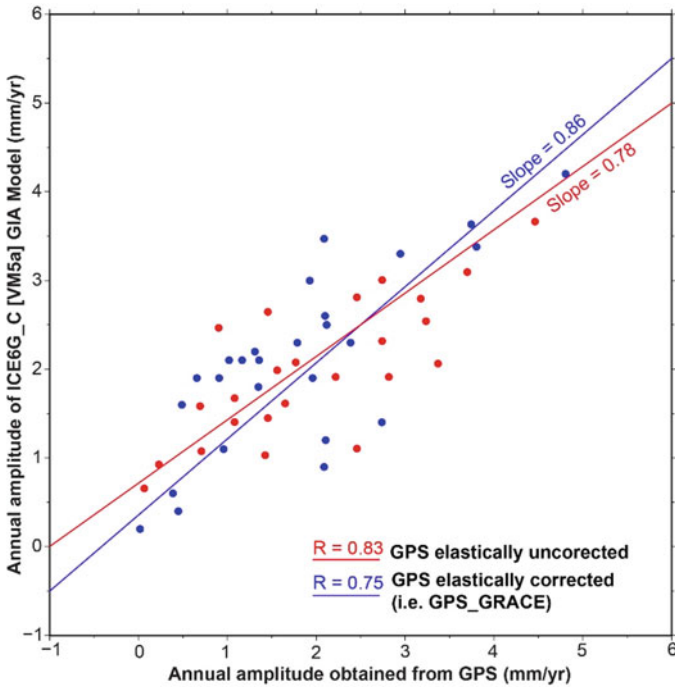


Fig. 7 Correlation plot between the annual amplitude estimated from the seasonal signals observed in GPS and elastically corrected GPS signals with the annual amplitude of the GIA model ICE6G_C [VM5a]. Red and blue lines indicate the estimated best fit line to the GPS elastically uncorrected and elastically corrected linear fit with slope and correlation coefficient (R) values

corrected and uncorrected GPS vertical velocities show that the GIA model values agree well with elastically corrected (GPS—GRACE) site velocities.

References

- Altamimi Z, Collilieux X, Metivier L (2011) ITRF2008: An improved solution of the international terrestrial reference frame. *J Geod* 85(8):457–473. <https://doi.org/10.1007/s00190-011-0444-4>
- Argus DF, Heftin MB (1995) Plate motion and crustal deformation estimated with geodetic data from the global positioning system. *Geophys Res Lett* 22:1973–1976
- Argus DF, Peltier WR (2010) Constraining models of postglacial rebound using space geodesy: a detailed assessment of model ICE-5G (VM2) and its relatives. *Geophys J Int* 181:697–723
- Argus DF, Peltier WR, Drummond R, Moore AW (2014) The Antarctica component of post-glacial rebound model ICE-6G_C (VM5a) based on GPS positioning, exposure age dating of ice thicknesses, and relative sea level histories. *Geophys J Int* 198:537–563
- Behrendt J (1999) Crustal and lithospheric structure of the West Antarctic rift system from geophysical investigations: a review. *Global Planet Change* 23(1–4):25–44

- Bevis M, Kendrick E, Smalley R Jr, Ian D et al (2009) Geodetic measurements of vertical crustal velocity in West Antarctica and the implications for ice mass balance. *Geochem Geophys Geosys* 10:Q10005. <https://doi.org/10.1029/2009GC002642>
- Bohem J, Werl B, Schuh H (2006) Troposphere mapping functions for GPS and very long baseline interferometry from European Centre for Medium-Range weather forecasts operational analysis data. *J Geophys Res - Solid Earth* 111(B2):B2406
- Blewitt, G, Lavallée D (2002) Effect of annual signals on geodetic velocity. *J Geophys Res* 107(B7:ETG 9–1–ETG 9–11). <https://doi.org/10.1029/2001JB000570>
- Bouin M-N, Vigny C (2020) New constraints on Antarctic plate motion and deformation from GPS data. *J Geophys Res* 105-B12:28279–28293
- DeMets C, Gordon RG, Argus D, Stein S (1990) Current plate motions. *Geophys J Int* 101:425–478
- Denton G, Prentice ML, Burckle LH (1991) Cainozoic history of the Antarctic ice-sheet. In: Tingey RJ (ed) *Geology of Antarctica*. Oxford Univ Press, New York, pp 365–433
- Dietrich R, Rülke A, Ihde J et al (2004) Plate kinematics and deformation status of the Antarctic Peninsula based on GPS. *Glob Planet Ch* 42:313–321
- Farrell WE (1972) Deformation of the Earth by surface loads. *Rev Geophys* 10:761–797
- Gharavi S, Catherine JK, Ambikapathy A, Kumar A, Gahalaut VK (2017) Antarctica Plate Motion. *Proc Indian Natn Sci Acad* 83(2):437–440
- Groh A et al (2012) An investigation of glacial isostatic adjustment over the Amundsen Sea Sector, West Antarctica. *Global Planet Change* 98:45–53. <https://doi.org/10.1016/j.gloplacha.2012.08.001>
- Grunow AM (1993) New paleomagnetic data from the Antarctic Peninsula and their tectonic implications. *J Geophys Res*. <https://doi.org/10.1029/93JB01089>
- Hattori A, Aoyama Y, Okuno J, Doi K (2021) GNSS Observations of GIA-Induced Crustal Deformation in Lützow-Holm Bay, East Antarctica. *Geophys Res Lett* 48:e2021GL093479. <https://doi.org/10.1029/2021GL093479>
- Hayes DE (1991) Tectonics and age of the oceanic crust: circum-Antarctic to 30°S. In: Hayes DE (ed) *Marine geological and geophysical atlas of the circum-Antarctic to 30°S*. American Geophysical Union, Washington, D.e, pp 47–56
- Herring TA (2003) MATLAB Tools for viewing GPS velocities and time series. *GPS Solutions* 7(3):194–199. <https://doi.org/10.1007/s10291-003-0068-0>
- Herring TA (2005) GLOBK, Global Kalman filter VLBI and GPS analysis program, Version 10.2, Report, Department of Earth, Atmospheric and Planetary Sciences, Massachusetts Institute of Technology.
- Huybrechts P (1994) Formation and disintegration of the Antarctic ice sheet. *Ann. Glaciol.* 20:336–340
- King MA, Penna NT, Clarke PJ (2005) Validation of ocean tide models around Antarctica using onshore GPS and gravity data. *J Geophys Res* 110:B08401. <https://doi.org/10.1029/2004JB003390>
- King MA, Bingham RJ, Moore P, Whitehouse PL, Bentley MJ, Milne GA (2012) Lower satellite-gravimetry estimates of Antarctic sea-level contribution. *Nature* 491(7425):586
- King MA, Whitehouse PL, van der Wal W (2016) Incomplete separability of Antarctic plate rotation from glacial isostatic adjustment deformation within geodetic observations. *Geophys J Int* 204:324–330
- King RW, Bock Y (2005) Documentation of the GAMIT GPS Analysis Software, Massachusetts Institute of Technology.
- Li W, Li F, Zhang S, et al. (2019) An assessment of GIA solutions based on high-precision GNSS velocity field for Antarctica. *Solid Earth Discuss* [preprint]. <https://doi.org/10.5194/se-2019-101>
- Lemoine J-M, Bruinsma S, Gégout P, Biancale R, Bourgogne S (2013) Release 3 of the GRACE gravity solutions from CNES/CRGS. *Geophys Res Abstracts*. 15(EGU2013-11123):2013
- Morelli A, Danesi S (2004) Seismological imaging of the Antarctic continental lithosphere: a review. *Global and Plan Ch* 42(1–4):155–165
- Nikolaidis R (2002) Observation of geodetic and seismic deformation with the Global Positioning System. Ph.D. thesis Univ of Calif, San Diego San Diego

- Ohzono M, Tabei T, Doi K, Shibuya K, Sagiya T (2006) Crustal movement of Antarctica and Syowa based on GPS measurements. *Earth Planet Space* 58:795–804
- Swenson S, Chambers D, Wahr J (2008) Estimating geocenter variations from a combination of GRACE and ocean model output. *J Geophys Res - Solid Earth* 113:B8
- Tapley BD, Bettadpur S, Ries JC, Thompson PF, Watkins MM (2004) GRACE measurements of mass variability in the Earth System. *Science* 305(5683):503–505. <https://doi.org/10.1126/science.1099192>
- Ten Brink US, Hackney RI, Bannister S et al (1997) Uplift of the transantarctic mountains and the bedrock beneath the East Antarctic ice sheet. *J Geophys Res* 102(B12):27603–27621
- Thomas ID, King MA, Bentley MJ, Whitehouse PL, Penna NT, Williams SDP, et al. (2011) Widespread low rates of Antarctic glacial isostatic adjustment revealed by GPS observations. *Geophys Res Lett* 38(22). L22302. <https://doi.org/10.1029/2011GL049277>
- Thomas ID, King MA, Bentley MJ, Whitehouse PL et al (2011) Widespread low rates of Antarctic glacial isostatic adjustment revealed by GPS observations. *Geophys Res Lett* 38:L22302
- Tian Y (2011) iGPS: IDL tool package for GPS position time series analysis. *GPS Sol* 15(3): 299–303. <https://doi.org/10.1007/s10291-011-0219-7>
- Tregoning P, Ramillien G, McQueen H, Zwartz D (2009) Glacial isostatic adjustment and non stationary signals observed by GRACE. *J Geophys Res* 114:B06406. <https://doi.org/10.1029/2008JB006161>
- van Dam T (2010) NCEP derived 6 hourly, global surface displacements at 2.5×2.5 degree spacing. [Available at <http://geophy.uni.lu/ncep-loading.html>]
- van Dam T, Collilieux X, Wuite J, Altamimi Z, Ray J (2012) Nontidal ocean loading effects in GPS height time series. *J Geodyn* <https://doi.org/10.1007/s00190-012-0564-5>
- van Dam TM, Wahr JM (1987) Displacements of the Earth's surface due to atmospheric loading: Effects on gravity and baseline measurements. *J Geophys Res* 92(B2):1281–1286. <https://doi.org/10.1029/JB092iB02p01281>
- Velicogna I, Mohajerani Y, Landerer F, Mouginit J, Noel B, Rignot E, et al. (2020). Continuity of ice sheet mass loss in Greenland and Antarctica from the GRACE and GRACE follow-on missions. *Geophys Res Lett* 47(8):e2020GL87291. <https://doi.org/10.1029/2020GL87291>
- Wahr J, Molenaar M, Bryan F (1998) Time variability of the Earth's gravity field: Hydrological and oceanic effects and their possible detection using GRACE. *J Geophys Res* 103(B12):30205–30229. <https://doi.org/10.1029/98JB02844>
- Wdowinski S, Bock Y, Zhang J, Fang P, Genrich J (1997) Southern California permanent GPS geodetic array: Spatial filtering of daily positions for estimating coseismic and postseismic displacements induced by the 1992 Landers earthquake. *J Geophys Res* 102(B8):18057–18070. <https://doi.org/10.1029/97JB01378>
- Williams SDP, Moore P, King MA, Whitehouse PL (2014) Revisiting GRACE Antarctic ice mass trends and accelerations considering autocorrelation. *Earth Planet Sci Lett* 385:12–21
- Zanutta A, Negusini M, Vittuari L et al (2018) New geodetic and gravimetric maps to infer geodynamics of antarctica with insights on Victoria Land. *Remote Sens* 10:1608. <https://doi.org/10.3390/rs10101608>